Title

Offline Coupling of Asymmetrical Flow Field-Flow Fractionation and Capillary Electrophoresis for Separation of Extracellular Vesicles.

Journal

Analytical Chemistry, 94(41)

Authors

Gao, Ziting
Hutchins, Zachary
Li, Zongbo
et al.

Publication Date

2022-10-18

DOI

10.1021/acs.analchem.2c03550

Peer reviewed

HHS Public Access

Author manuscript

Anal Chem. Author manuscript; available in PMC 2023 October 18.

Published in final edited form as:

Anal Chem. 2022 October 18; 94(41): 14083–14091. doi:10.1021/acs.analchem.2c03550.

Offline Coupling of Asymmetrical Flow Field-Flow Fractionation and Capillary Electrophoresis for Separation of Extracellular Vesicles

Ziting Gao,
Department of Chemistry, University of California—Riverside, Riverside, California 92521, United States

Zachary Hutchins,
Department of Chemistry, University of California—Riverside, Riverside, California 92521, United States

Zongbo Li,
Department of Chemistry, University of California—Riverside, Riverside, California 92521, United States

Wenwan Zhong
Department of Chemistry, University of California—Riverside, Riverside, California 92521, United States

Abstract

Extracellular vesicles (EVs) play important roles in cell-to-cell communications and carry high potential as markers targeted in disease diagnosis, prognosis, and therapeutic development. The main obstacles to EV study are their high heterogeneity; low amounts present in samples; and physical similarity to the abundant, interfering matrix components. Multiple rounds of separation and purification are often needed prior to EV characterization and function assessment. Herein, we report the offline coupling of asymmetrical flow field-flow fractionation (AF4) and capillary electrophoresis (CE) for EV analysis. While AF4 provides gentle and fast EV separation by size, CE resolves EVs from contaminants with similar sizes but different surface charges. Employing Western Blotting, ELISA, and SEM, we confirmed that intact EVs were eluted within a stable time window under the optimal AF4 and CE conditions. We also proved that EVs could be resolved from free proteins and high-density lipoproteins by AF4 and be further separated from the low-density lipoproteins co-eluted in AF4. The effectiveness of the coupled AF4-CE system in

Corresponding Author: Wenwan Zhong – Department of Chemistry, University of California—Riverside, Riverside, California 92521, United States; wenwan.zhong@ucr.edu.

Supporting Information

The Supporting Information is available free of charge at https://pubs.acs.org/doi/10.1021/acs.analchem.2c03550.
Additional method description; electropherograms of standard EVs in different running conditions; SEM images of standard EVs, EVs collected from different CE running conditions and EVs eluted from AF4 with the the injection of 100 μL of HeLa cell medium; EV recovery from membrane filtration; AF4 fractograms and CE electropherograms of EV-free medium, HeLa cell medium with and without treatment at 12, 24, and 48 h, and human serum by AF4-CE, and direct injections of culture media and serum by AF4 or CE alone (PDF)

Complete contact information is available at: https://pubs.acs.org/10.1021/acs.analchem.2c03550

The authors declare no competing financial interest.

EV analysis was demonstrated by monitoring the changes in EV secretion from cells and by direct injection of human serum and detection of serum EVs. We believe that coupling AF4 and CE can provide rapid EV quantification in biological samples with much reduced matrix interference and be valuable for the study of total EVs and EV subpopulations produced by cells or present in clinical samples.

Graphical Abstract

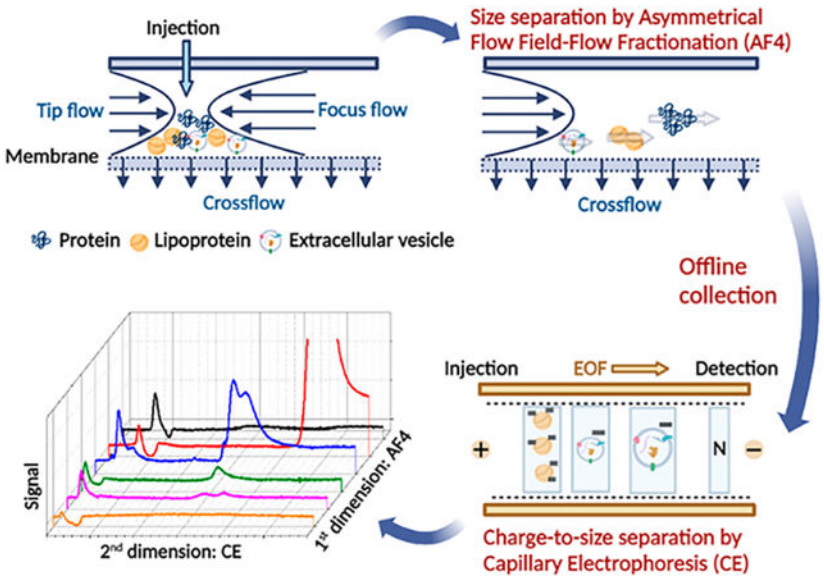

INTRODUCTION

Extracellular vesicles (EVs) secreted from almost all types of cells have sizes ranging from 30 to 200 nm and are easily accessible in all body fluids.[1] EVs carry cargos that include nucleic acids, metabolites, lipids, proteins, etc.[2] Some of these cargos are believed to carry out specific functions once taken up by recipient cells,[3] and some are reflective of their cells of origin depending on the EV biogenesis pathway.[4] These features of EVs demonstrate their high potential as disease markers and therapeutic targets, drawing tremendous research efforts to gain a better understanding of EV functions and biogenesis. Advanced analytical technologies are thus demanded to permit rapid but accurate inspection of EVs present in biological samples.

However, rapid EV analysis is not easy. EVs are highly heterogeneous. A variety of EV subpopulations are different in many aspects, including biogenesis pathways, physical sizes, and molecular components;[5] and they can carry out different functions.[6] Additionally, the low number of EVs secreted by cells could be too diluted in the culture medium; or, in clinical studies, only a limited volume of biofluids is available, in which the EVs at low quantities could be masked by the highly abundant matrix components and become undetectable.[7] Many strategies have been widely adopted for EV separation, including ultracentrifugation (UG) or differential centrifugation,[8] ultrafiltration (UF),[9] immuno-affinity capture (IAC),[10] size-exclusion chromatography (SEC),[11] and polymer-

based precipitation.[12] However, the heterogeneous EVs cannot be simply distinguished by only one property, like one surface marker, size, density, or surface hydrophobicity,[13] and it is difficult to completely remove the abundant matrix components. Therefore, it is hard to use one separation technique to obtain EVs with high purity for accurate quantification, not to mention to resolve different EV subpopulations. Besides, these processes are often labor-intensive and time-consuming and require large amounts of samples.[14] Advanced microfluidic devices have also been constructed and demonstrated for streamlined EV separation,[15] but they are technically demanding and not yet easily adaptable in common biomedical research or clinical laboratories.

New column-based separation methods have been reported to speed up EV isolation with enhanced purity, like the polyester capillary-channeled polymer fiber column that separates EVs from impurities by hydrophobic interaction.[16] Still, packed columns may present concerns over EV integrity due to potential collision with column packing during separation. An open-channel separation technique, asymmetrical flow field-flow fractionation (AF4), has attracted increasing attention for EV purification. AF4 separates analytes based on their sizes using two perpendicular liquid flows: the channel flow and the crossflow. Under the normal elution mode, smaller molecules migrate faster than bigger ones because of their higher diffusion coefficients.[17,18] AF4 can accommodate analytes falling within a wide size range, including biological macromolecules, nano- and microparticles, vesicles, and cells, with one separation channel but different flow programs. The instrument also provides gentle separation to maintain sample integrity to a large extent because there is no concern about collision with column packing.[19] These features make AF4 highly suitable for EV separations.[1,14,20–23] AF4 is viewed to provide good resolution over a much wider particle size range and superior flexibility compared to SEC and can provide higher purity and integrity of the isolated EVs than UG and UF methods.[3,14]

Flow rates in AF4 are quite large, causing significant dilution of the injected samples and requiring a postseparation enrichment step to enhance the concentration of the eluted EVs for downstream analysis.[14,20,22] Moreover, it is very difficult for AF4 to resolve EVs from low-density lipoproteins (LDLs) because they share similar sizes,[24] and resolution would get worse with samples containing high protein concentrations that may overload the column. Thus, AF4 methods for EV separation typically work with the relatively clean samples treated by UG or UF. To improve separation resolution, capillary electrophoresis (CE) is no doubt one of the best choices. CE has also demonstrated excellent separation power over labeled or UG-enriched EVs,[25–27] but no CE methods reported so far can directly analyze EVs from complex biofluids like serum with sufficient resolution, since the highly abundant proteins and lipids in such samples would produce enormous peaks that cover up the signal from EVs. We hypothesize that coupling AF4 with CE can overcome the challenges in EV separation from complex matrices faced by using AF4 or CE alone. AF4 can separate EVs from the smaller, abundant contaminants, quickly reducing the sample complexity; CE can resolve the roughly cleaned EVs from the impurities with similar sizes and not separable in AF4, enabling accurate EV quantification. Herein, we developed and applied the AF4-CE method for rapid quantification of EVs present in cell culture medium and human serum. We demonstrated that offline coupling of AF4 and CE is able to monitor secretion of EVs from cells by directly sampling the culture medium and to detect the EVs in human serum with

significantly reduced interference from the abundant proteins and lipoproteins. Besides rapid EV quantification, we believe this system should also be useful for obtaining purified EV subpopulations for downstream molecular profiling.

EXPERIMENTAL SECTION

Reagents and Materials.

Purified EVs (lyophilized exosomes from human colon carcinoma cell line COLO-1) were purchased from HansaBioMed Life Science Ltd. (Tallinn, Estonia). High-density lipoprotein (HDL) and low-density lipoprotein (LDL) were obtained from CalBioChem (EMD Millipore, Billerica, MA). Pooled human serum samples were purchased from Innovative Research, Inc. (Novi, MI). Glycine (G8898-500G, ≥99%), bromophenol blue sodium salt (B8026-5G), DMEM - high glucose (SH30243.01), Anti-CD81 antibody (SAB4700232-100UG), albumin (A9511-500MG, ≥97%), and IgG (I4506-10MG, ≥95%) were from Sigma-Aldrich (St. Louis, MO). Phosphate buffered saline (PBS), 10× solution (AAJ75889K8, molecular biology grade; consisting of 80.6 mM sodium phosphate, 19.4 mM potassium phosphate, 27 mM KCl, and 1.37 M NaCl in high-purity deionized H_2O), FL-70 (SF105-1), sodium azide (S227I-100, ≥99%), NaOH (S318-500, 97.0%), HCl (A144-500, 36.5 to 38.0%), Tris base (BP152-500, ≥99.8%), SDS (BP8200500, > 99%), DTT (BP172-5, ≥99%), glycerol (PRH5433, ≥ 99.5%), penicillin-streptomycin (15140122, 100×), and GW4869 (501873728) were purchased from Fisher Scientific (Fairlawn, NJ).

AF4 Separation and Fraction Enrichment.

An AF2000 system manufactured by Postnova Analytics (Salt Lake City, UT) was used in this study. The trapezoidal separation channel spacer was 0.350 mm. The injection loop volume was 150 μL. The regenerated cellulose ultrafiltration membrane (Postnova Analytics) with a 10 kDa molecular weight cutoff (MWCO) was used for separation. The running buffer for all samples was 0.1× PBS (100-fold dilution of the purchased 10× PBS stock) containing 0.1% FL-70 and 0.02% sodium azide. The use of FL-70 and 10 kDa RC provides a stable elution profile and an acceptable size accuracy.[28] Fractograms were recorded by an SPD-20A absorbance detector (Shimadzu), and the eluates were collected by a fraction collector (BIO-RAD). The AF4 separation method started with a 5 min focusing step, using a crossflow at 3.00 mL/min, a tip flow at 0.30 mL/min, and a focus flow at 2.90 mL/min. After focusing, a 1 min transition step was employed where the focus flow was reduced to zero, and then the tip flow was increased to 3.20 mL/min with crossflow going down to 2.00 mL/min. Following this, the tip flow was linearly reduced to 0.20 mL/min within 20 min, with the detector flow kept at 0.20 mL/min and crossflow gradually decreasing to zero. The fraction collection was performed at every 2 min interval. These 2 min collections were then concentrated to 15 μL by filtration using the 100 kDa MWCO Amicon Ultra Centrifugal Filter (Millipore Sigma). The injection volume varied from sample to sample. For culture medium analysis, we did three repeated injections of 100 μL of medium to AF4, and we combined all of the eluates from the same collection window for filtration. For serum separation, to avoid protein overloading, we used only a small injection volume of 10 μL without any repeated injections.

CE Separation and Fraction Collection.

CE separation was conducted in an Agilent 7100 CE system (equipped with a UV absorption detector and a data acquisition system of ChemStation), using a bare fused silica capillary (Polymicro Technologies) with an inner diameter of 50 μm, an outer diameter of 365 μm, and a total/effective length of 35/26.5 cm. The injection was performed at 50 mbar for 10 s. Typically, a separation voltage of 10 kV and a background electrolyte of 0.5× PBS (20-fold dilution of the stock 10× PBS) were employed, except during method optimization. All CE traces were recorded by measuring with the UV absorption at the wavelength of 200 nm. Before each day's experiment, the capillary was flushed with 0.5 M NaOH, 0.1 M HCl, and H_2O. For fraction collection, samples were continuously injected into the system at least 8 times and fractions were collected based on the migration window of the targets of interest.

EV Characterization by Nanoparticle Tracking Analysis (NTA), Scanning Electron Microscopy (SEM), Enzyme-Linked Immunosorbent Assay (ELISA), and Western Blotting (WB).

HeLa cells were cultured in Gibco DMEM (high glucose) containing 10% FBS (Bio-Techne) and 1% penicillin-streptomycin at 37 °C in a humidified 5% CO_2 incubator (Thermo Electron Corporation). EVs were harvested, and EV secretion affected by the treatment of GW4869 was also inspected. The EVs collected from the culture media by UG were counted by NanoSight NS300 (Malvern Instruments). SEM analysis was performed with an NNS450 instrument (ThermoFisher Scientific). The EVs were immobilized on the silica wafer and coated with a cPt/Pd sputter coater prior to SEM measurement. EV protein analysis by ELISA was done in 96-well plates, using anti-CD9 (Millipore Sigma) and anti-CD81 for EV capture and the biotinylated anti-CD63 (BioLegend) and the streptavidin-conjugated horseradish peroxidase (HRP) for EV detection. Chemiluminescence produced by HRP was read at a BioTek Synergy H1 Hybrid Multi-Mode Microplate Reader. WB was performed in a BIO-RAD gel electrophoresis and membrane transfer system; anti-CD63 (Novus Biologicals), anti-ApoA (Novus Biologicals), and anti-ApoB (Novus Biologicals) were used for recognition of target proteins. The HRP-conjugated goat-antimouse IgG (Invitrogen) and HRP-conjugated goat-antirabbit IgG (Promega) were employed as the secondary antibodies. The membranes were imaged by an Odyssey XF Imaging System (LI-COR Biosciences). The detailed conditions for cell culture, EV harvest, and EV characterization can be found in the Supporting Information.

Data Analysis.

All quantitation data was collected with multiple biological repeats and are presented as the means ± S.D. Statistical significance was calculated by unpaired two-tailed Student's *t* test using GraphPad Prism 8.0.

RESULTS AND DISCUSSION

EV Separation and Quantification by CE.

We first confirmed the capability of CE in EV separation and quantification. In consideration of the potential damage to the fragile vesicles from the strong electric field and Joule heating, we focused our method development on selection of the background electrolytes (BGE) and the separation voltage, aiming to maintain good EV integrity while achieving sufficient resolution. We tested the most common biological buffer, phosphate buffered saline, and diluted the stock 10× PBS at 100, 20, and 10 fold to obtain 1×, 0.5×, and 0.1× PBS, respectively. The buffer of 10 mM phosphate with no additional salt (PB, pH 7.4) was also included. For each BGE, the separation voltages of 10, 20, and 30 kV were evaluated. The purchased standard EVs were resuspended in pure water according to the manufacturer's guidelines and injected during method optimization.

From the electropherograms (Figure S1), we can see that reproducible migration times (RSD ranging from 2% to 10%) were obtained in all separation conditions. Higher separation voltages resulted in shorter EV elution times, which also decreased with increasing salt content in the BGE because of reduction of the electroosmotic flow (EOF). We also found that a negative peak consistently showed up before the EV peak in 1× or 0.5× PBS, which became positive in 0.1× PBS and PB. The elution time of this peak was the same as that of the neutral compound DMSO if injected, indicating that it could be the injection peak resulting from the electrolyte composition difference between the sample solution (containing unrevealed chemicals in the lyophilized powder received from the supplier) and the BGE. The EVs migrated later than the "neutral" peak under the positive electric field mode, indicating the EV lipid membranes should carry negative charges.

Using the injection peak as the "neutral marker", we calculated the electrophoretic mobility (μ_{ep}) of the EVs (Figure 1A). The μ_{ep} was the most negative, i.e., with the largest absolute value ($|\mu_{ep}|$), in 10 mM PB, the one with the lowest salt content. It is possible that the salt content suppressed formation of the electrical double layer on the vesicle surface, reducing their electrophoretic mobility. But, in the BGE prepared from different dilutions of PBS, the mobility became more negative with higher salt content, i.e., $|\mu_{ep}|_{1\times PBS} > |\mu_{ep}|_{0.5\times PBS} > |\mu_{ep}|_{0.1\times PBS}$. We suspected vesicle size increase in the lower salt content BGE may play a role in the decrease of the $|\mu_{ep}|$ value. Surprisingly, we found that μ_{ep} measured in the same BGE varied with the separation voltage, with the minimal change observed in 1× PBS. In addition, we measured the peak area and normalized it against the migration time to correct for the difference in the transit time through the detection window.[29] We noticed that the largest normalized CE peak areas were achieved in 0.5× PBS with a separation voltage of 10 and 20 kV (Figure 1B). Large variations were found in the normalized peak area with the no-salt PB as the BGE, and the BGE of 0.1× PBS resulted in the lowest normalized area. These results suggest that the EVs must have experienced certain damage when the migration was driven by a high electric field and/or with a salt content much lower than the physiological condition. There was also visible peak area reduction along with increasing separation voltage in 1× PBS. The higher Joule heating in such a high-salt buffer may have caused some damage to the EVs, decreasing the amounts of the intact EVs.[30]

To further reveal the changes occurring to EVs, we collected the eluate from the EV peak obtained with the separation voltage of 10 kV in 0.5× PBS, and with 30 kV in 10 mM PB. We inspected the collected EVs by SEM. We understand SEM may not be as ideal as cryogenic transmission electron microscopy (Cryo-TEM)[31] or as TEM with negative or positive staining for inspection of the vesicle structures. But our purpose was to observe the potential vesicle damage, morphology change, or occurrence of aggregation caused by CE separation, and SEM, which is easier to perform, should be sufficient for this purpose. Still, to maintain the morphological features and reduce the damage to EVs when being examined in the vacuum chamber of the SEM instrument, the EVs were chemically immobilized on the SEM wafer surface prior to dehydration (Supporting Information).[32] Indeed, the SEM images exhibit significant aggregation and deformation of the EVs when separated with 30 kV in 10 mM PB (Figure S2C), while the EVs eluted at 10 kV in 0.5× PBS maintained the spherical shape observed before the CE separation and showed no aggregation (Figure S2A,B). The aggregated EVs and potential vesicle debris resulting from EV deformation may contribute to the sharp peak proceeding to the EV peak observed in 0.1× PBS or 10 mM phosphate.

The following CE tests were then all done with a separation voltage of 10 kV in 0.5× PBS, because it resulted in the most reproducible and largest peak area among all conditions tested and eluted EVs with good morphology and little aggregation. Using 0.5× PBS as the BGE may also lead to the effect of field-amplified sample stacking when we analyzed EVs dissolved in a buffer with a lower electrolyte concentration, which could help stack the injected EVs at the boundary between the sample plug and the running buffer, giving sharper peaks and improved signal-to-noise ratios.[33]

Serial dilutions of the standard EVs were injected and separated by the optimal condition, i.e., in 0.5× PBS with 10 kV. The EVs were eluted at consistent migration times (Figure 1C), the peak area linearly increasing with the EV input (R^2 = 0.9916). As low as 8.7 × 10^6 particles/μL EVs can be detected, calculated using the 3σ method (Figure 1D). This LOD is comparable to that reported by CE-LIF with the EVs stained by membrane-bound dyes.[25] CE is not as sensitive as NTA and ELISA,[34,35] two common techniques used for EV quantification; however, ELISA is time-consuming and NTA can quantify only highly purified EVs.[36,37] CE also provides the benefit of low sample consumption and good reproducibility. Overall, our results well support the possibility of using CE to quantify the EVs eluted by AF4 in the following study.

EV Separation by AF4 and Sample Enrichment after AF4.

We chose AF4 as the first separation dimension in our 2D design because it can handle injection up to several hundred microliters and can resolve the EVs from the abundant impurities with smaller sizes. These features are beneficial if a sample with a very complex matrix or a large volume is under investigation. With AF4 initially resolving the EVs from components of different sizes, the fractionated EVs can enter the second separation dimension, i.e., CE, with low amounts of contaminants to prevent overloading in CE. The co-eluted contaminants with similar sizes can also be well resolved from the EVs, permitting accurate quantification.

The AF4 method was adopted from our previous work.[23] The EVs should be eluted after 20 min with this method. We injected 100 μL of 10^9 standard EVs or the DMEM culture medium with 10% FBS, but we did not observe any obvious peaks in the UV–vis detector (Figure 2A) except for a huge peak appearing at around 10 min from injection of the culture medium. This peak should be from proteins like albumin.[23] We collected the eluate from AF4 separation of the culture medium until the crossflow cutoff time, i.e., 26 min, and found the average particle size increases with elution time, agreeing with the normal elution mode in AF4 (Figure 2D). However, WB only found CD63 in the fraction collected between 22 and 24 min (designated as F2, Figure 2C). CD63 is a tetraspanin marker of exosomes,[38] one family of EVs carrying high potential as disease markers. The vesicles collected in the other two fractions, i.e., F1 (20–22 min) and F3 (24–26 min), may have a lower content of CD63 below the detection limit of WB or could belong to other EV families like microvesicles that are not detectable by the anti-CD63 antibody. This result reflects that even heterogeneous EVs were present in this purchased “EV standard”. The sizes of the particles found in F1 were in general smaller than those present in F2, agreeing with their elution orders in AF4, and particles with an irregular shape were observed in F3, which could be from membrane debris present in the culture medium or microvesicles (Figure S2D,E).

With a detector flow rate of 0.20 mL/min, the eluate collected within a 2 min elution window yields a volume of 0.40 mL, and the concentration of the eluted compounds could be too diluted to be detected in CE. A quick and efficient enrichment step should be taken before the AF4 fraction can be analyzed by CE. UG and lyophilization are possible ways to precipitate the EVs and other components so that the excess liquid can be removed; however, both take several hours or even overnight to complete. We chose to use the ultrafiltration membrane filters with large molecular weight cut-off (MWCO) values, i.e., 30, 100, and 300 kDa. Their pore sizes are small enough that EVs with diameters larger than 30 nm cannot pass through and large enough to permit rapid filtration: they took less than 10 min to reduce the fraction volume from 400 to 15 μL. We evaluated the recovery using ELISA and NTA for EV quantification. Our ELISA protocol captures the EVs by the surface markers of CD81 and CD9 and detects the presence of CD63 on the EVs. Thus, it only detects intact vesicles eluted in AF4 and enriched by filtration, rather than free proteins from vesicle debris. NTA counts the number of particles recovered in the filtrate. Both results showed that the filter with a 100 kDa MWCO value gave out the highest EV recovery among all filters tested and recovered ~100% EVs from the AF4 eluate (Figure S3A).

Next, the fractions collected from separation of 10^9 standard EVs (the supplier claims this sample contains mainly exosomes) by AF4 were concentrated using the 100 kDa MWCO filter, and the enriched filtrate was injected to CE, with the resultant electropherograms shown in Figure 2B. Agreeing with the WB result, in this EV sample, only F2 showed a peak in the elution time (6–8 min) comparable to that found with direct injection and CE analysis of the standard EVs (Figure 1C). Injection of F3 exhibited multiple low-intensity peaks in later elution times, consistent with the SEM results that presented particles with irregular shapes and possibly vesicle or cell membrane debris. The electropherogram of F1 also showed a peak eluted between 6 and 8 min but with a much lower signal than that found in F2, which could be the same types of EVs carrying comparable charge-to-size ratios as those eluted in F2 although their sizes are relatively smaller. Another peak was detected

at an earlier elution time of ~5 min, supporting that the EV particles eluted in the same AF4 fraction could exhibit a difference in electrophoretic mobility. Because their sizes are comparable, i.e., unresolvable by AF4, these vesicles are possibly different in their surface properties, highlighting the necessity of developing a high-resolution, hyphenated system that can target different EV properties in EV analysis to obtain detailed information about the EV subpopulations in samples.

AF4-CE for Monitoring EV Secretion by HeLa Cells.

Study of EV functions often requires frequent inspection of EV secretion from cells or tissues stimulated by various factors or undergoing pathological or physiological transitions. Typically, EV secretion analysis would start with the lengthy step of EV purification from the culture medium, followed by the empirical particle counting or the more specific detection of EV markers. A large number of cells (at least 10^6–10^7 cells) need to be cultured, and a large volume of culture medium is to be collected, enhancing the difficulties in the study of EV secretion from cells that may not be cultured easily and readily available in a high amount, like primary cells or stem cells.

We anticipated that our AF4-CE platform is a valuable tool for monitoring EV quantity change with little sample consumption and thus suitable to monitor EV secretion from cells under different conditions. To prove this, we applied our system to analyze EV secretion from HeLa cells. We prepared the EV-free medium by combining both filtration and UG. We confirmed that negligible EVs were detected in the EV-free medium by AF4-CE before EV collection (Figure S4A), unless it was spiked with a number of the standard EVs (Figure S4B). Then, we collected the medium at 12, 24, and 48 h after putting the cells in the EV-free medium. Of the 30 mL of medium collected, 300 μL was directly analyzed by AF4-CE, and the rest was treated by UG to enrich sufficient EVs for ELISA. The CE results showed that the EV peak area increased gradually from 12, 24, to 48 h in all three AF4 fractions (electropherograms from F2 are displayed in Figure 3A; bar plots for EV peak areas are shown in Figure 3C, red bars; and results from all other fractions are in Figure S5), and the changes were statistically significant ($p < 0.05$). These results clearly show that more and more EVs were secreted by the cells with a longer culturing time. We also confirmed the CE results using ELISA: by normalizing the peak area or ELISA signal against that from the 12 h collection, we observed the same increasing trend of the EV amount collected at 12, 24, and 48 h between the results from AF4-CE and ELISA (Figure 3D).

In addition, we treated the cells with 10 μM GW4869, a potent neutral inhibitor that prevents the formation of intraluminal vesicles (ILVs) and blocks exosome production,[39] and analyzed the culture media collected at 0, 12, 24, and 48 h after the treatment by AF4-CE (Figures 3B and S6). The EV concentrations in the culture media were calculated using the resultant EV peak areas, and the calibration curve was obtained using standard EVs (Figure 3C, blue bars). While EV secretion still increased along with the culturing duration, it was significantly suppressed by GW4869. Spiking the standard EVs into the F2 fraction collected from the 48 h treatment, we further confirmed the EV elution time (the purple trace in Figure 3B).

In this study, AF4-CE used only 300 μL of culture medium for three repeated injections while 3 mL of medium was needed to collect enough EVs for ELISA, and the total time for AF4-CE is within 2 h compared to the 2–3 days needed for UG-based EV purification followed by ELISA-based EV quantification. We also attempted direct injection to AF4 or CE. As shown in Figure S7, the low-concentration EVs in the unprocessed medium could not be detected by the UV–vis detector. Direct injection to CE also showed negligible signal in the EV elution window (6–8 min) but large peaks were shown before 6 min with no detectable changes over different culturing times (the purple trace in Figures 3A and S8) were observed. These results strongly support that AF4-CE permits continuous monitoring of EV secretion from cells by sampling a small volume of the culture medium and carrying out rapid EV quantification, which cannot be achieved by running AF4 or CE alone.

AF4-CE for Analysis of EVs in Human Serum.

Biofluids collected from patients, like serum and plasma, are the subjects of examination during marker discovery and validation. They are much more complex than cell culture media and often contain highly abundant matrix components difficult to be resolved from EVs using one single technique. For instance, we found that the elution window for the LDL complexes spanned from 18 to 26 min (the blue trace in Figure 4A), overlapping with that of the EVs. It has been well-known that the size of LDL and very low-density lipoprotein (VLDL) could range from 20 to 200 nm,[40] comparable to EVs. On the other hand, AF4 can well resolve EVs from HDL, albumin, and IgGs (Figure 4A, the green, orange, and black traces, respectively). These components are very abundant and cannot even be completely removed from the EVs precipitated by UG (the red trace in Figure 4A). On the other hand, under the CZE condition we employed, IgG was eluted within a comparable time as the standard EVs, while LDL, HDL, and albumin were eluted at later times (Figure 4B). These preliminary tests support the feasibility of using AF4-CE to analyze the EV quantities in biofluids because AF4 can remove the highly abundant proteins and resolve EVs from HDLs, while CE can separate EVs from LDLs that are co-eluted with EVs in AF4.

Similar to the results found with culture medium analysis, direct injection of 10 or 25 μL of serum to AF4 or the 10× diluted serum to CE could not lead to satisfactory separation results nor was it able to clearly identify the EV elution peaks in either separation (Figures 5A, S9, and S10A). Analysis of the serum components eluted in AF4 using WB revealed that HDL (represented by the detection of ApoA) was eluted within 12–14 min and LDL (represented by the detection of ApoB) was found from 15 to 26 min (Figure 5B). Interestingly, in serum samples, CD63 was also detected in earlier fractions, i.e., from 12 to 20 min. We carried out ELISA on these fractions and detected intact vesicles in F1, F2, and F3, but not in the fractions collected from 15 to 20 min, proving that the CD63 signal detected in these fractions was from the free protein (Figure 5C). But a relatively high amount of intact EVs was also found in 12–14 min. Direct injection of the undiluted serum may have caused column overloading, and some EVs leaked out during the focusing step.

These fractions were also inspected by CE. A large peak was eluted after 8 min in most of the fractions, which could be LDL by comparing this elution with that from the standard LDL (Figure 4). The fractions collected between 15 and 20 min also exhibited large peaks

within the EV elution window, which could be from the free proteins. Much cleaner electropherograms were attained from F1, F2, and F3, the EV eluting fractions. Spiking the standard EVs to the samples confirmed that the small peak eluted at around 6 min should be the EVs (Figure S10B). These results demonstrate that AF4-CE is capable of analyzing EVs in highly complex samples. We also noticed that in serum, the larger EVs eluted in F3 were at a lower abundance and different peak shape than those in F1 and F2, unlike what was observed in the cell culture media study (Figure 5D). This observation hints that the size distribution profiles of EVs present in different samples could be different and highlights the importance of separating different EV subpopulations by more diverse properties, like size plus surface charge, rather than a single property.

CONCLUSIONS

Here, we have shown that AF4-CE is an effective method of separating and quantifying EVs in complex biological samples. This system is capable of continuously monitoring EV secretion by directly sampling from culture media and can separate the EVs from the abundant matrix components like proteins and lipoproteins based on sizes as well as charge-to-size ratios. The combination of two separation techniques allows high separation resolution, despite the minimal size differences between some lipoproteins and EVs. AF4-CE is rapid and requires small sample consumption as shown by tens of microliters of injections, reducing sample consumption and analysis time. It is also versatile, as a large variety of biofluids can be applied and EV quantification can be done without labeling. All these features make AF4-CE an excellent tool for EV analysis, which should also benefit analysis of other types of bioparticles such as viruses and bacteria in complex matrices.

Certainly the current off-line coupling of AF4 and CE still needs to be improved for more effective EV analysis. For example, the CE mode employed in the present work is CZE, which has a very limited loading capacity. Electrophoretic preconcentration, such as capillary isoelectric focusing[41–43] or large-volume sample stacking,[44] could be considered to permit injection of more of the collected AF4 eluate in CE and to enhance EV detection sensitivity. In addition, we anticipate that the EVs with different sizes can be separated by AF4, and those with similar sizes but different in their surface charges can be further resolved in CE. The capability to inject a large amount of EVs to the CE dimension after AF4 can then make it possible to collect the EVs eluted from CE for molecular profiling using various omics tools[45,46] or single vesicle detection methods,[47] which will improve our understanding of the biogenesis and functions of different EV subpopulations.

Supplementary Material

Refer to Web version on PubMed Central for supplementary material.

ACKNOWLEDGMENTS

Research reported in this publication was supported by UCR's Extramural Funding Opportunity Preparation Award (EFOPA) and City of Hope – UC Riverside Biomedical Research Initiative (CUBRI) to W. Zhong. Electron microscopy was performed on a scanning electron microscope NNS450 instrument in the Central Facility for Advanced Microscopy and Microanalysis (CFAMM) at UC Riverside, with the assistance of Dr. Ilkum Lee. The schematic graphic in the table of contents and abstract graphic was created with BioRender.com.

REFERENCES

(1). Cocozza F; Grisard E; Martin-Jaular L; Mathieu M; Théry C Cell 2020, 182, 262–262.e1. [PubMed: 32649878]

(2). van Niel G; D'Angelo G; Raposo G Nat. Rev. Mol. Cell Biol 2018, 19, 213–228. [PubMed: 29339798]

(3). Doyle LM; Wang MZ Cells 2019, 8, 727. [PubMed: 31311206]

(4). Dickhout A; Koenen RR Front. Cardiovasc. Med 2018, 5, 113. [PubMed: 30186839]

(5). Gould SJ; Raposo GJ Extracell. Vesicles 2013, 2, 20389.

(6). Allelein S; Medina-Perez P; Lopes ALH; Rau S; Hause G; Kölsch A; Kuhlmeier D Sci. Rep 2021, 11, 11585. [PubMed: 34079007]

(7). Sherman CD; Lodha S; Sahoo S Cells 2021, 10, 1500. [PubMed: 34203713]

(8). Théry C; Amigorena S; Raposo G; Clayton A Curr. Protoc. Cell. Biol 2006, 30, 3.22.21–23.22.29.

(9). Di Giuseppe F; Carluccio M; Zuccarini M; Giuliani P; Ricci-Vitiani L; Pallini R; De Sanctis P; Di Pietro R; Ciccarelli R; Angelucci S Biomedicines 2021, 9, 146. [PubMed: 33546239]

(10). Campos-Silva C; Suárez H; Jara-Acevedo R; Linares-Espinós E; Martinez-Piñeiro L; Yáñez-Mó M; Valés-Gómez M Sci. Rep 2019, 9, 2042. [PubMed: 30765839]

(11). Gámez-Valero A; Monguió-Tortajada M; Carreras-Planella L; Franquesa M. l.; Beyer K; Borràs FE Sci. Rep 2016, 6, 33641. [PubMed: 27640641]

(12). Niu Z; Pang RTK; Liu W; Li Q; Cheng R; Yeung WSB PloS one 2017, 12, e0186534. [PubMed: 29023592]

(13). Busatto S; Yang Y; Iannotta D; Davidovich I; Talmon Y; Wolfram JJ Extracell. Vesicles 2022, 11, e12202.

(14). Zhang H; Lyden D Nat. Protoc 2019, 14, 1027–1053. [PubMed: 30833697]

(15). Guo S-C; Tao S-C; Dawn HJ Extracell. Vesicles 2018, 7, 1508271.

(16). Huang S; Ji X; Jackson KK; Lubman DM; Ard MB; Bruce TF; Marcus RK Anal. Chim. Acta 2021, 1167, 338578. [PubMed: 34049630]

(17). Contado C Anal. Bioanal. Chem 2017, 409, 2501–2518. [PubMed: 28116495]

(18). Kowalkowski T; Buszewski B; Cantado C; Dondi F Crit. Rev. Anal. Chem 2006, 36, 129–135.

(19). Fraunhofer W; Winter G Eur. J. Pharm. Biopharm 2004, 58, 369–383. [PubMed: 15296962]

(20). Kim YB; Yang JS; Lee GB; Moon MH Anal. Chim. Acta 2020, 1124, 137–145. [PubMed: 32534666]

(21). Sitar S; Kejžar A; Pahovnik D; Kogej K; Tušek-Žnidarič M; Lenassi M; Žagar E Anal. Chem 2015, 87, 9225–9233. [PubMed: 26291637]

(22). Kim YB; Lee GB; Moon MH Anal. Chem 2022, 94, 8958–8965. [PubMed: 35694825]

(23). Ashby J; Flack K; Jimenez LA; Duan Y; Khatib A-K; Somlo G; Wang SE; Cui X; Zhong W Anal. Chem 2014, 86, 9343–9349. [PubMed: 25191694]

(24). German JB; Smilowitz JT; Zivkovic AM Curr. Opin. Colloid Interface Sci 2006, 11, 171–183. [PubMed: 20592953]

(25). Morani M; Mai TD; Krupova Z; Defrenaix P; Multia E; Riekkola M-L; Taverna M Anal. Chim. Acta 2020, 1128, 42–51. [PubMed: 32825911]

(26). Ouahabi OE; Salim H; Pero-Gascon R; Benavente FJ Chromatogr. A 2021, 1635, 461752.

(27). Piotrowska M; Ciura K; Zalewska M; Dawid M; Correia B; Sawicka P; Lewczuk B; Kasprzyk J; Sola L; Piekoszewski W; et al. J. Chromatogr. A 2020, 1621, 461047. [PubMed: 32197757]

(28). Maknun L; Sumranjit J; Siripinyanond A RSC Adv 2020, 10, 6423–6435. [PubMed: 35495991]

(29). Altria KD Chromatographia 1993, 35, 177–182.

(30). Rathore AS J. Chromatogr. A 2004, 1037, 431–443. [PubMed: 15214680]

(31). Bordanaba-Florit G; Royo F; Kruglik SG; Falcón-Pérez JM Nat. Protoc 2021, 16, 3163–3185. [PubMed: 34135505]

(32). Nanou A; Crespo M; Flohr P; De Bono JS; Terstappen LWMM Cancers 2018, 10, 416. [PubMed: 30384500]

(33). Osbourn DM; Weiss DJ; Lunte CE Electrophoresis 2000, 21, 2768–2779. [PubMed: 11001283]

(34). Yang Z; Atiyas Y; Shen H; Siedlik MJ; Wu J; Beard K; Fonar G; Dolle JP; Smith DH; Eberwine JH; et al. Nano Lett 2022, 22, 4315–4324. [PubMed: 35588529]

(35). Park J; Park JS; Huang C-H; Jo A; Cook K; Wang R; Lin H-Y; Van Deun J; Li H; Min J; et al. Nat. Biomed. Eng 2021, 5, 678–689. [PubMed: 34183802]

(36). Lai JJ; Chau ZL; Chen S-Y; Hill JJ; Korpany KV; Liang N-W; Lin L-H; Lin Y-H; Liu JK; Liu Y-C; et al. Adv. Sci 2022, 9, 2103222.

(37). Bachurski D; Schuldner M; Nguyen P-H; Malz A; Reiners KS; Grenzi PC; Babatz F; Schauss AC; Hansen HP; Hallek M; et al. J. Extracell. Vesicles 2019, 8, 1596016. [PubMed: 30988894]

(38). Kim D.-k.; Nishida H; An SY; Shetty AK; Bartosh TJ; Prockop DJ Proc. Natl. Acad. Sci. U. S. A 2016, 113, 170–175. [PubMed: 26699510]

(39). Catalano M; O'Driscoll LJ Extracell. Vesicles 2020, 9, 1703244.

(40). Wojczynski MK; Glasser SP; Oberman A; Kabagambe EK; Hopkins PN; Tsai MY; Straka RJ; Ordovas JM; Arnett DK Lipids Health Dis 2011, 10, 181. [PubMed: 22008512]

(41). Xu T; Han L; Sun L Anal. Chem 2022, 94, 9674–9682. [PubMed: 35766479]

(42). Fonslow BR; Kang SA; Gestaut DR; Graczyk B; Davis TN; Sabatini DM; Yates JR Iii Anal. Chem 2010, 82, 6643–6651. [PubMed: 20614870]

(43). Martinović S; Berger SJ; Paša-Tolić L; Smith RD Anal. Chem 2000, 72, 5356–5360. [PubMed: 11080887]

(44). He Y; Lee HK Anal. Chem 1999, 71, 995–1001. [PubMed: 21662769]

(45). Haraszti RA; Didiot M-C; Sapp E; Leszyk J; Shaffer SA; Rockwell HE; Gao F; Narain NR; DiFiglia M; Kiebish MA; et al. J. Extracell. Vesicles 2016, 5, 32570. [PubMed: 27863537]

(46). Turchinovich A; Drapkina O; Tonevitsky A Transcriptome of Extracellular Vesicles: State-of-the-Art. Front. Immunol 2019, 10. DOI: 10.3389/fimmu.2019.00202

(47). Guo K; Li Z; Win A; Coreas R; Adkins GB; Cui X; Yan D; Cao M; Wang SE; Zhong W Biosens. Bioelectron 2021, 192, 113502. [PubMed: 34298496]

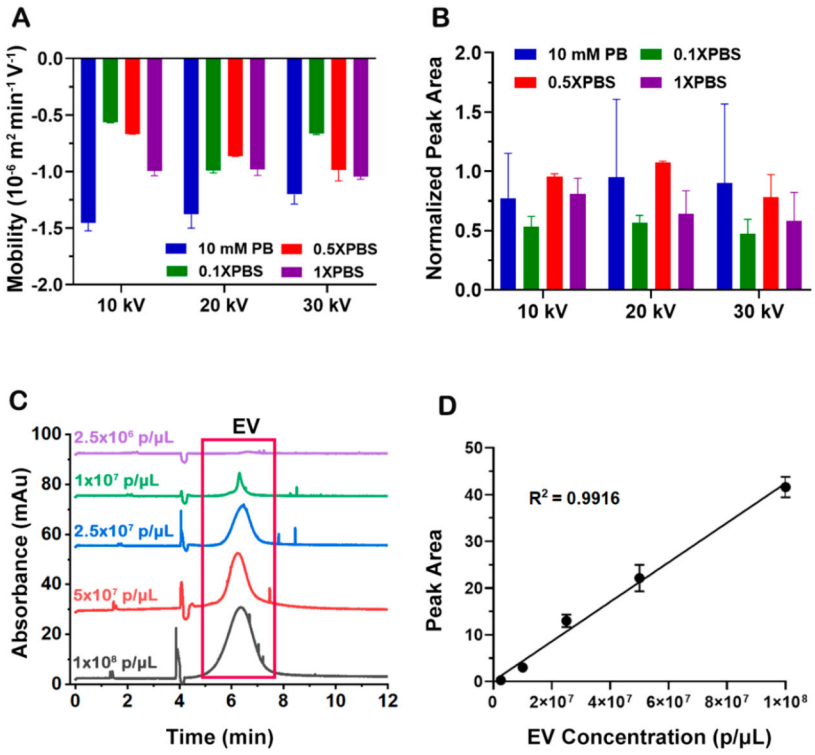

Figure 1.

(A) Electrophoretic mobility of EVs at various running conditions. (B) Comparison of the CE normalized peak areas acquired at various CE running conditions. (C) Electropherograms of standard EVs injected with different concentrations at the optimal running conditions, i.e. using 0.5× PBS as the BGE and 10 kV as the separation voltage, with the EV peaks highlighted in a red rectangle. (D) Calibration curve of CE peak areas versus EV concentrations.

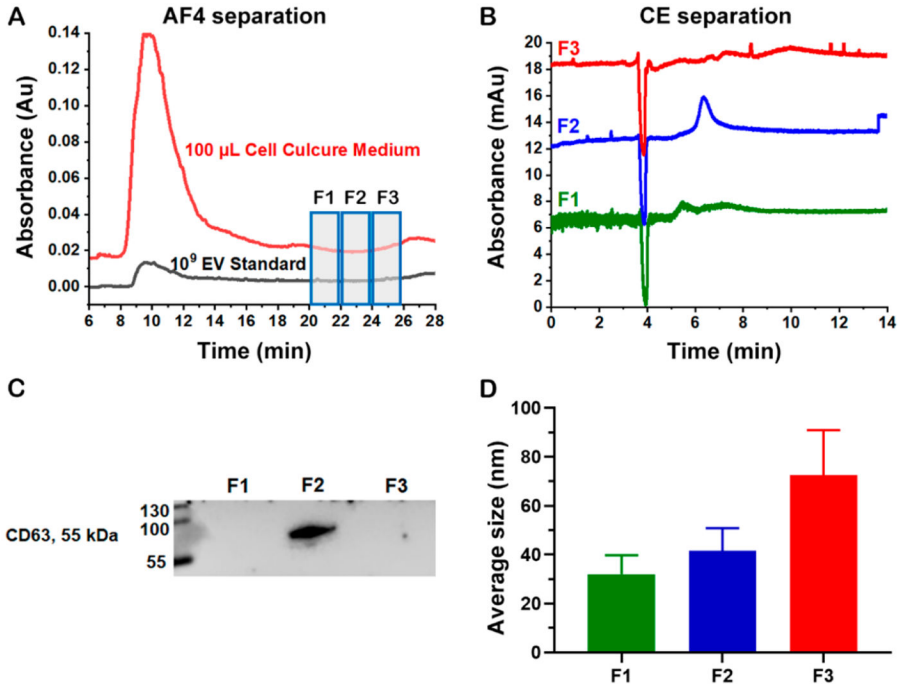

Figure 2.

(A) Fractograms of injecting 100 μL of HeLa cell medium (red trace) and 10^9 standard EVs (black trace) to AF4. (B) CE traces of three AF4 fractions were collected from injection of 10^9 standard EVs. F1: 20–22 min; F2: 22–24 min; and F3: 24–26 min (green, blue, and red traces, respectively). (C) WB analysis of CD63 protein, an EV marker, in three AF4 fractions collected from injection of 100 μL of HeLa cell medium. (D) Average diameter of the particles (a total of 15–20 particles counted in each fraction) in the AF4 fractions collected from HeLa cell medium observed in SEM images (images shown in Figure S2D,E).

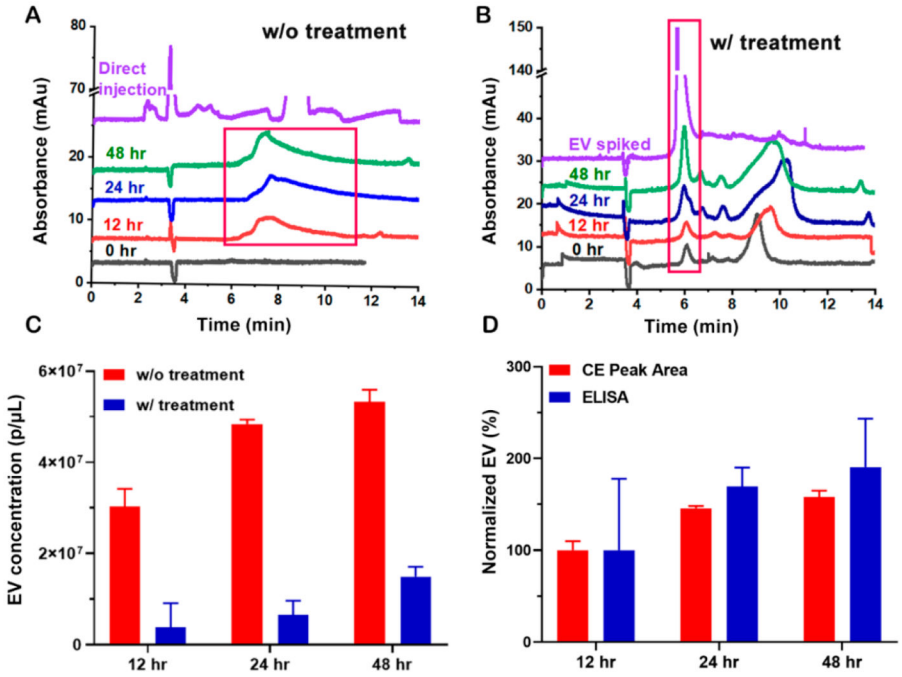

Figure 3.

(A and B) Electropherograms of the F2 fraction from AF4 separation of the culture media collected at 0, 12, 24, and 48 h harvesting time, with the cells treated (B) or untreated (A) by GW4869. The EV peaks are highlighted in red rectangles. The purple trace in panel A is the CE result from direct injection of the sample collected at the 12 h time point, and that in panel B is the electropherogram of the F2 fraction as used in the green trace but spiked with the EV standard. (C) EV concentrations with or without chemical treatment were calculated from the EV peak areas in CE using the titration curves obtained with EV standards. The concentration was the sum of the EVs eluted in all three AF4 fractions. (D) Increase of the total EV quantity in the culture media along with increasing harvesting time, with the quantity (from all three AF4 fractions) obtained by CE and ELISA and normalized against the signal collected at 12 h. The samples were collected from untreated cells.

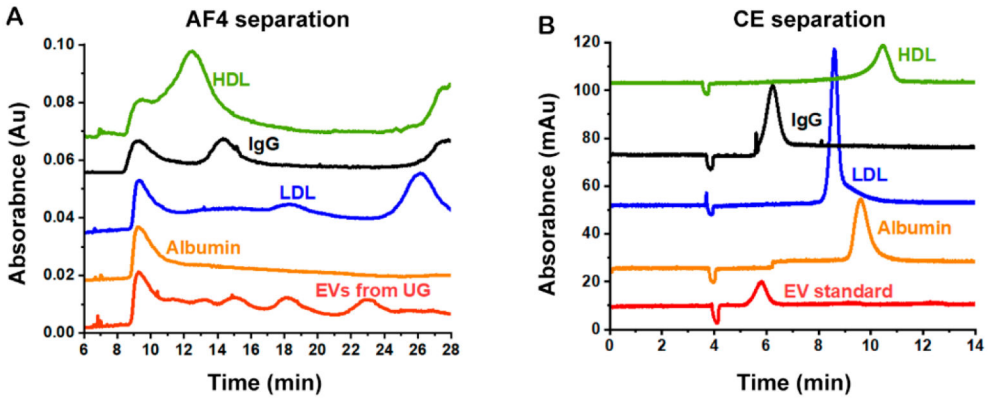

Figure 4.

(A) AF4 fractograms of HDL, IgG, LDL, albumin, and EVs collected from UG. (B) CE electropherograms of HDL, IgG, LDL, albumin, and EV standard.

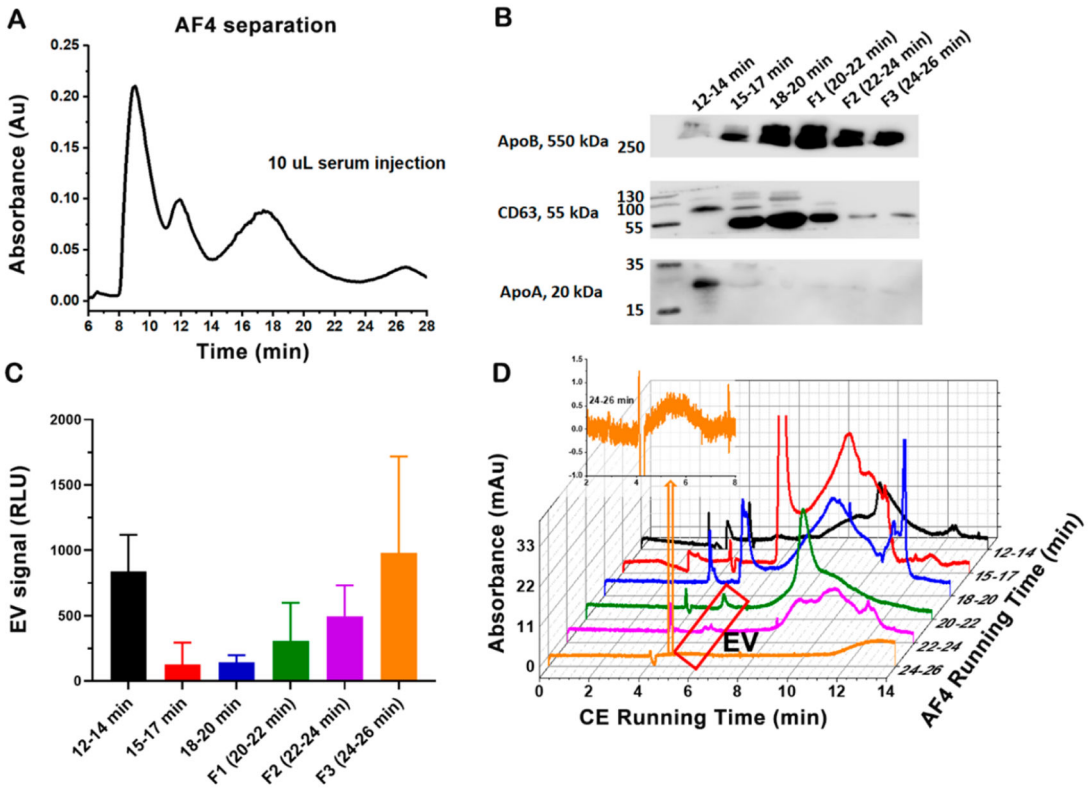

Figure 5.

(A) AF4 fractograms of 10 μL of pooled human serum. (B) Western blot analysis of CD63 protein, ApoB (an LDL marker), and ApoA (an HDL marker) in the 6 AF4 fractions collected from injection of 10 μL of pooled human serum. (C) ELISA results for quantification of EVs in the 6 AF4 fractions collected from injection of 25 μL of pooled human serum. (D) Electropherograms of the 6 AF4 fractions collected from injection of 10 μL of pooled human serum with the EV peak in F3 enlarged. The red rectangle encloses the EV peaks detected in the F1–F3 fractions.